



A Trilateral Weighted Sparse Coding Scheme for Real-World Image Denoising

Jun Xu¹, Lei Zhang¹, David Zhang^{1,2}

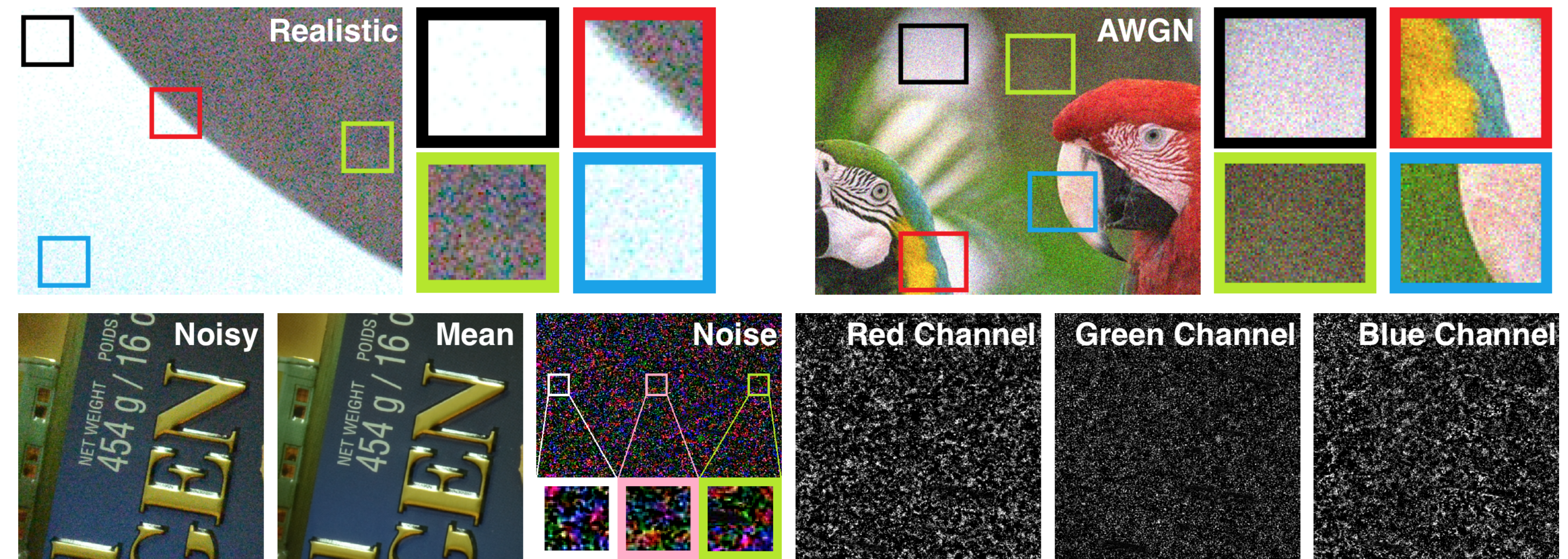
¹ Department of Computing, Hong Kong Polytechnic University, Hong Kong SAR, China

² School of Science and Engineering, The Chinese University of Hong Kong (Shenzhen), Shenzhen, China

Problem, Motivation, and Contributions

Goal: Estimating the latent clean image from the input real-world noisy image.

Motivation: Realistic noise show channel-wise and locally signal dependent property.



Contributions:

- Propose a trilateral weighted sparse coding (TWSC) scheme for real-world denoising;
- TWSC achieves much better performance than state-of-the-art denoising methods.

The TWSC Scheme

TWSC: Given a color image patch $\mathbf{Y} = \mathbf{X} + \mathbf{N} \in 3p^2 \times N$ and $\mathbf{Y} = \mathbf{DSV}^\top$ is the SVD of \mathbf{Y} . The TWSC model can be written as

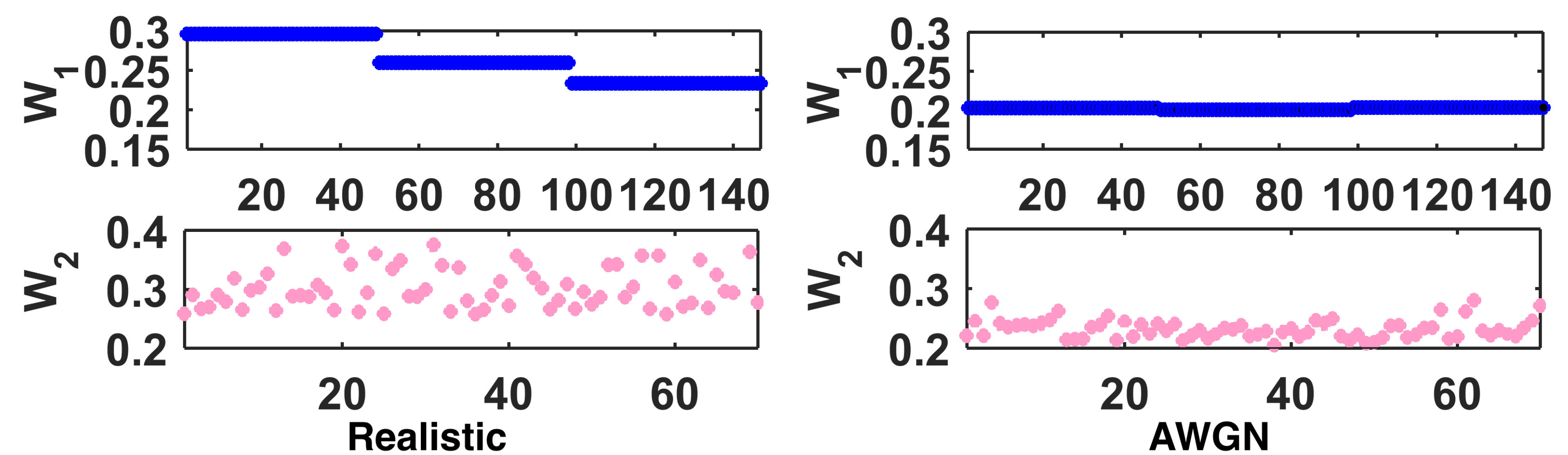
$$\hat{\mathbf{C}} = \arg \min_{\mathbf{C}} \|\mathbf{W}_1(\mathbf{Y} - \mathbf{DC})\mathbf{W}_2\|_F^2 + \|\mathbf{W}_3^{-1}\mathbf{C}\|_1. \quad (1)$$

The estimation of \mathbf{X} can be $\hat{\mathbf{X}} = \mathbf{D}\hat{\mathbf{C}}$.

Formulation of weight matrices:

$$\begin{aligned} \mathbf{W}_1 &= \text{diag}(\sigma_r^{-1/2}\mathbf{I}_{p^2}, \sigma_g^{-1/2}\mathbf{I}_{p^2}, \sigma_b^{-1/2}\mathbf{I}_{p^2}), \\ \mathbf{W}_2 &= \text{diag}(\sigma_1^{-1/2}, \dots, \sigma_M^{-1/2}), \mathbf{W}_3 = \mathbf{S}, \end{aligned} \quad (2)$$

Visualization of weight matrices:



Optimization

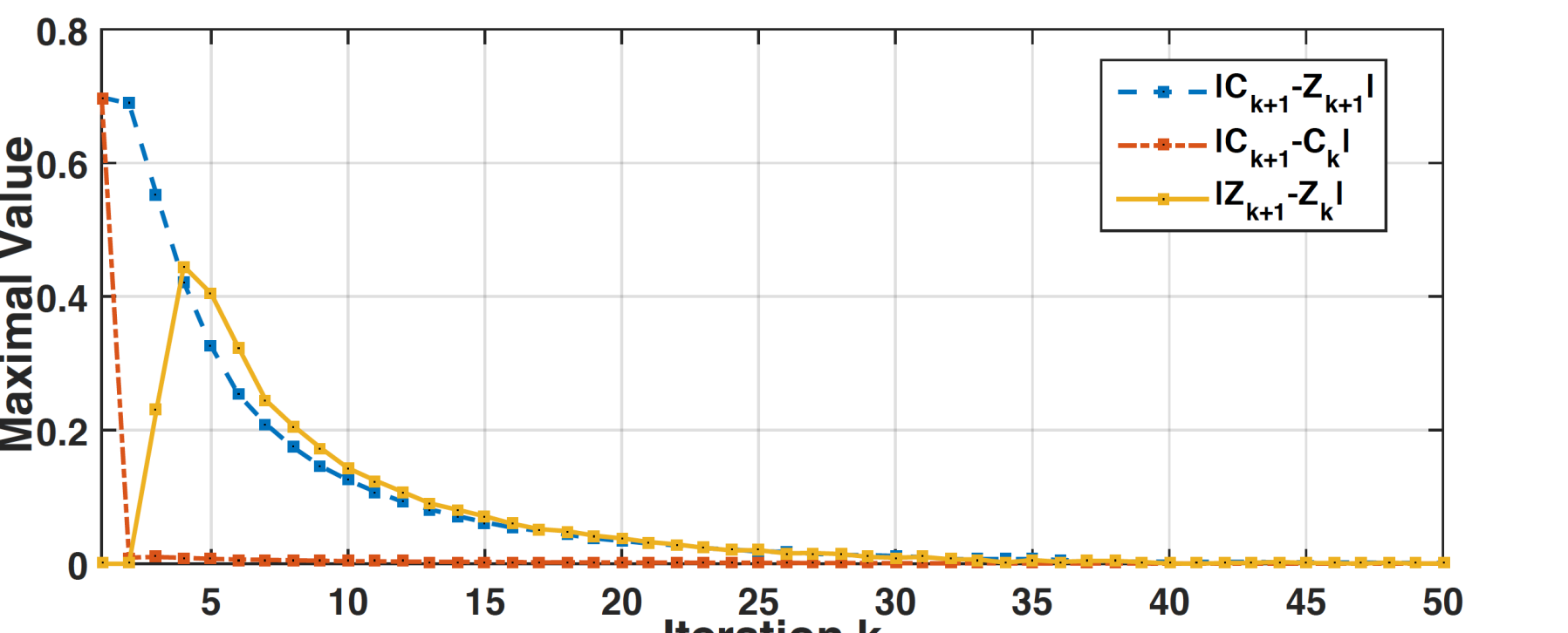
Variable Splitting: $\min_{\mathbf{C}, \mathbf{Z}} \|\mathbf{W}_1(\mathbf{Y} - \mathbf{DW}_3\mathbf{C})\mathbf{W}_2\|_F^2 + \|\mathbf{Z}\|_1$ s.t. $\mathbf{C} = \mathbf{Z}$.

ADMM:

- $\mathbf{C}_{k+1} = \arg \min_{\mathbf{C}} \|\mathbf{W}_1(\mathbf{Y} - \mathbf{DW}_3\mathbf{C})\mathbf{W}_2\|_F^2 + \frac{\rho_k}{2}\|\mathbf{C} - \mathbf{Z}_k + \rho_k^{-1}\Delta_k\|_F^2$.
The solution \mathbf{C}_{k+1} satisfies $\mathbf{AC}_{k+1} + \mathbf{C}_{k+1}\mathbf{B}_k = \mathbf{E}_k$, where $\mathbf{A} = \mathbf{W}_3^\top \mathbf{D}^\top \mathbf{W}_1^\top \mathbf{W}_1 \mathbf{D} \mathbf{W}_3$, $\mathbf{B}_k = \frac{\rho_k}{2}(\mathbf{W}_2 \mathbf{W}_2^\top)^{-1}$, $\mathbf{E}_k = \mathbf{W}_3^\top \mathbf{D}^\top \mathbf{W}_1^\top \mathbf{W}_1 \mathbf{Y} + (\frac{\rho_k}{2}\mathbf{Z}_k - \frac{1}{2}\Delta_k)(\mathbf{W}_2 \mathbf{W}_2^\top)^{-1}$.
(Solution) $\mathbf{C}_{k+1} = \text{vec}^{-1}((\mathbf{I}_M \otimes \mathbf{A} + \mathbf{B}_k^\top \otimes \mathbf{I}_{3p^2})^{-1} \text{vec}(\mathbf{E}_k))$.
Challenge: Is $(\mathbf{I}_M \otimes \mathbf{A} + \mathbf{B}_k^\top \otimes \mathbf{I}_{3p^2})^{-1}$ exist?
- $\mathbf{Z}_{k+1} = \arg \min_{\mathbf{Z}} \frac{\rho_k}{2}\|\mathbf{Z} - (\mathbf{C}_{k+1} + \rho_k^{-1}\Delta_k)\|_F^2 + \|\mathbf{Z}\|_1$.
- $\Delta_{k+1} = \Delta_k + \rho_k(\mathbf{C}_{k+1} - \mathbf{Z}_{k+1})$.
- $\rho_{k+1} = \mu\rho_k$, where $\mu \geq 1$.

Theoretical Analysis

Convergence:



Existence of the Solution to ADMM (a):

Theorem 1. Assume that $\mathbf{A} \in \mathbb{R}^{3p^2 \times 3p^2}$, $\mathbf{B} \in \mathbb{R}^{M \times M}$ are both symmetric and positive semi-definite matrices. If at least one of \mathbf{A}, \mathbf{B} is positive definite, the Sylvester equation $\mathbf{AC} + \mathbf{CB} = \mathbf{E}$ has a unique solution for $\mathbf{C} \in \mathbb{R}^{3p^2 \times M}$.

Corollary 1. The **Solution** to ADMM (a) exists and is unique.

Experimental Results

Quantitative Comparisons on AWGN Removal:

Table 1: Average results of PSNR(dB) and SSIM of different denoising algorithms on 20 grayscale images corrupted by AWGN noise.

| σ_n | Metric | BM3D-SAPCA | LSSC | NCSR | WNNM | TNRD | DnCNN | WSC | TWSC |
|------------|--------|------------|--------|--------|--------|--------|--------|--------|--------|
| 15 | PSNR | 32.42 | 32.27 | 32.19 | 32.43 | 32.27 | 32.59 | 32.06 | 32.34 |
| | SSIM | 0.8860 | 0.8849 | 0.8814 | 0.8841 | 0.8815 | 0.8879 | 0.8673 | 0.8846 |
| 25 | PSNR | 30.02 | 29.84 | 29.76 | 30.05 | 29.87 | 30.22 | 29.57 | 29.98 |
| | SSIM | 0.8364 | 0.8329 | 0.8293 | 0.8365 | 0.8314 | 0.8415 | 0.8179 | 0.8372 |
| 35 | PSNR | 28.48 | 28.26 | 28.17 | 28.51 | 28.33 | 28.66 | 28.01 | 28.49 |
| | SSIM | 0.7969 | 0.7908 | 0.7855 | 0.7958 | 0.7907 | 0.8021 | 0.7765 | 0.7987 |
| 50 | PSNR | 26.85 | 26.64 | 26.55 | 26.92 | 26.75 | 27.08 | 26.35 | 26.93 |
| | SSIM | 0.7481 | 0.7405 | 0.7391 | 0.7499 | 0.7415 | 0.7563 | 0.7258 | 0.7530 |
| 75 | PSNR | 24.74 | 24.77 | 24.66 | 25.15 | 24.97 | 25.24 | 24.54 | 25.15 |
| | SSIM | 0.6649 | 0.6746 | 0.6793 | 0.6903 | 0.6801 | 0.6931 | 0.6612 | 0.6949 |

Quantitative Comparisons on Realistic Noise Removal:

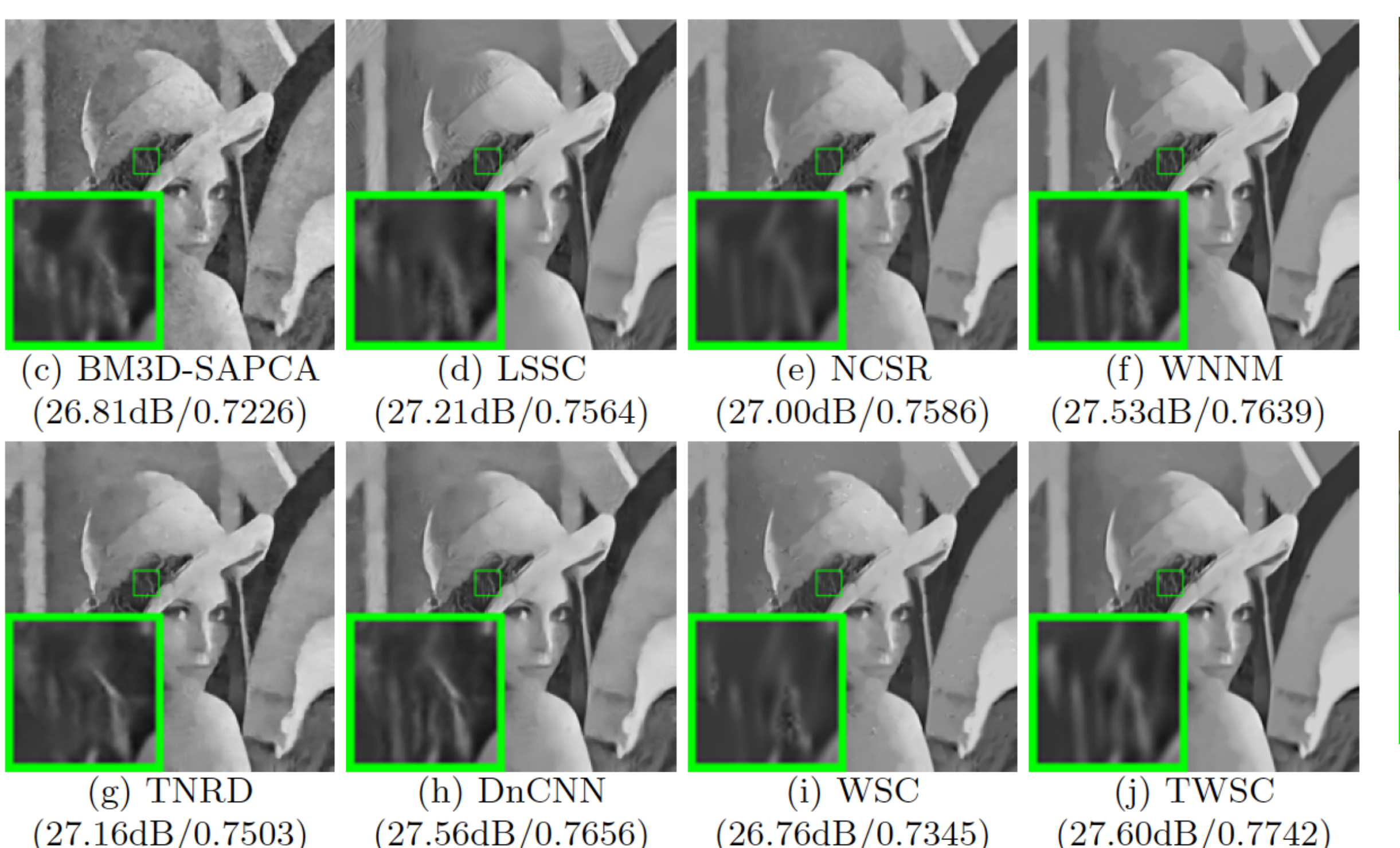
Table 2: Average results of PSNR(dB) and SSIM of different denoising methods on 15 cropped real-world noisy images used in [24].

| | CBM3D | TNRD | DnCNN | NI | NC | CC | MCWNNM | WSC | TWSC |
|------|--------|--------|--------|--------|--------|--------|--------|--------|---------------|
| PSNR | 35.19 | 36.61 | 33.86 | 35.49 | 36.43 | 36.88 | 37.70 | 37.36 | 37.81 |
| SSIM | 0.8580 | 0.9463 | 0.8635 | 0.9126 | 0.9364 | 0.9481 | 0.9542 | 0.9516 | 0.9586 |

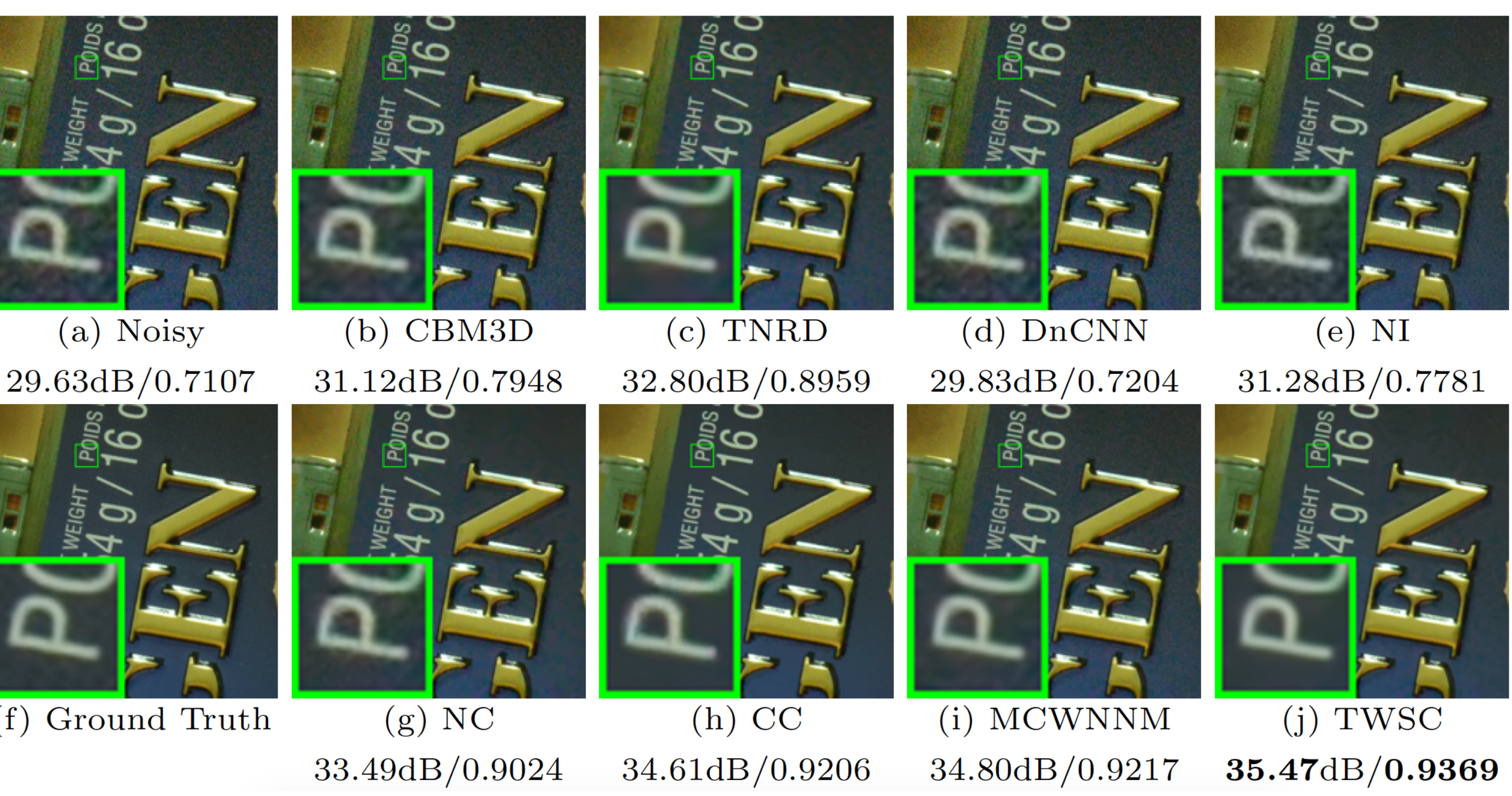
Table 3: Average results of PSNR(dB) and SSIM of different denoising methods on 1000 cropped real-world noisy images in [29].

| | CBM3D | TNRD | DnCNN | NI | NC | MCWNNM | WSC | TWSC |
|------|--------|--------|--------|--------|--------|--------|--------|---------------|
| PSNR | 32.14 | 34.15 | 32.41 | 35.11 | 36.07 | 37.38 | 36.81 | 37.94 |
| SSIM | 0.7773 | 0.8271 | 0.7897 | 0.8778 | 0.9013 | 0.9294 | 0.9165 | 0.9403 |

Comparisons on Lena (AWGN with $\sigma = 75$):



Comparisons on Nikon D800 ISO 6400 1 in CC dataset [24]:



Quantitative Results on Speed:

Table 4: Average computational time (s) of different methods to process a 512×512 image in the DND dataset [29].

| | CBM3D | TNRD | DnCNN | NI | NC | MCWNNM | WSC | TWSC |
|------|-------|------|-------|-----|------|--------|-------|-------|
| Time | 6.9 | 5.2 | 79.5 | 1.1 | 15.6 | 208.1 | 188.6 | 195.2 |

